One-dimensional Transient Heat Conduction Problem in a Plane Wall

MASTER'S DEGREE IN THERMAL ENGINEERING

GIADA ALESSI

Problem Specification

A large homogeneous wall whose geometry and physical properties are given in the table 1, is in contact with a fluid medium in its left-hand side ($x = 0$).

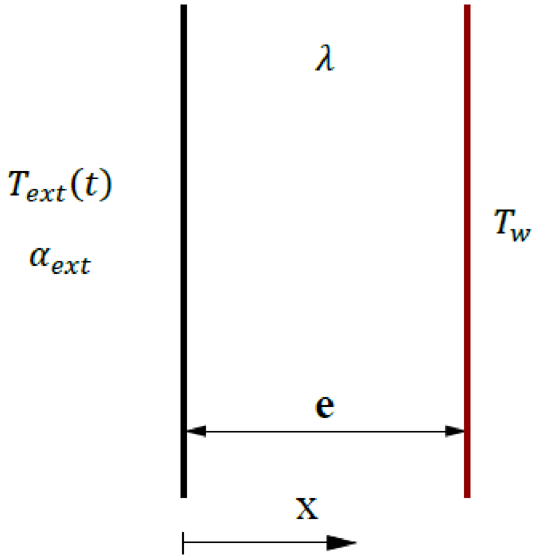

Figure 1. General scheme of the proposed problem.

The heat transfer coefficient α_{ext} can be considered constant, but the temperature of the medium changes following the law:

$$T_{ext}(t) = A_o + A_1 \sin(\omega_1 t) + A_2 \sin(\omega_2 t)$$

Where t is time in seconds and ω_1, ω_2 are:

$$\omega_1 = \frac{2\pi}{24 \cdot 3600} \qquad \omega_2 = \frac{2\pi}{365 \cdot 24 \cdot 3600}$$

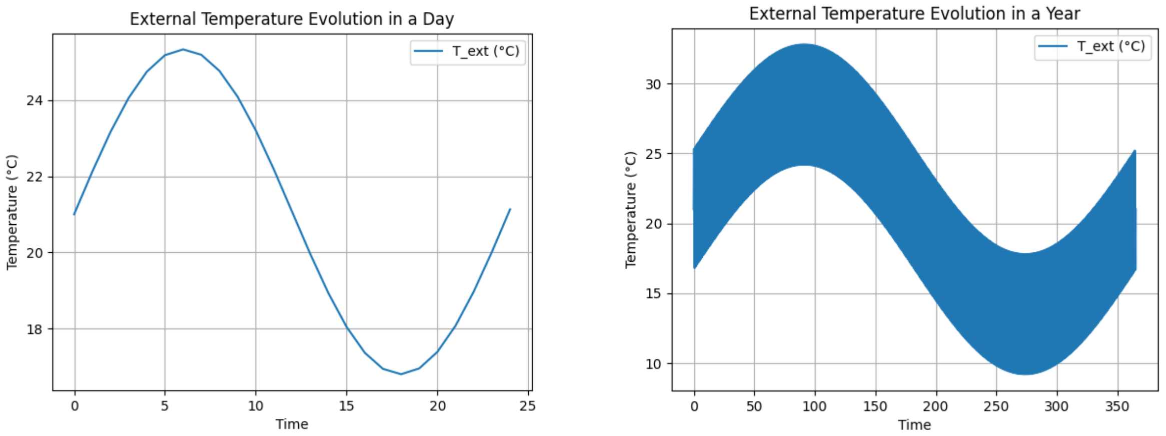

Figure 2. External temperature evolution during a single day (left) and a year (right).

The temperature of the plate on its right-hand side ($x = e$) is kept constant at $T = T_w$. The initial temperature of the wall is $T = T_0$. *Table 1* gives the physical parameter of this problem.

Table 1. Physical parameters of the given problem.

e $[m]$	ρ $\left[\frac{kg}{m^3}\right]$	c_p $\left[\frac{J}{kgK}\right]$	λ $\left[\frac{W}{mK}\right]$	α_{ext} $\left[\frac{W}{m^2K}\right]$	T_o $[°C]$	A_o $[°C]$	A_1 $[°C]$	A_2 $[°C]$	T_w $[°C]$
1.0	2400	900	220	8.7	21.0	21.0	4.3	7.5	21.0

Numerical Methodology and Code Structure

The problem has been solved implementing a Python code that models the transient heat conduction in the wall using the finite volume method.

Code Structure

The code has been structured as follows:

- **Input Data**
  - Definition of dimensions and thermal properties (conductivity, density, specific heat) of the wall. Definition of external temperature T_{ext} parameters, initial temperature T_0 of the wall and fixed temperature at the end of it, T_w.
  - Definition of numerical data used to solve the problem, N number of control volumes, time step Δt, time frame Int, tolerance δ, relaxation factor ω, and β parameter to define the integration scheme.

- **Domain Discretization**

  The wall has been divided into N control volumes using the finite volume method. Each control volume is represented by a node at the center and two additional nodes are positioned at the boundaries. Each node and control volume position have been evaluated considering a uniform mesh with uniform spacing.

- **Definition of Vectors**

  Bi-dimensional vectors were defined to store temperatures at each node and each time step, energy and time vectors were generated for energy balances and to plot graphs. Additionally, the initial temperature field has been set at T_0 in all the domain.

- **Unsteady Schemes**

  A generic formulation has been implemented to allow to change the β parameter and see how the program reacts to the three different schemes. The governing energy balance equation is applied for each control volume and is needed to evaluate the discretization coefficient.

$$\rho_P v_p \bar{c}_{p_P}(T_P^{n+1} - T_P^n) = \left\{\beta \sum \dot{Q}_P^{n+1} + (1-\beta) \sum \dot{Q}_P^n\right\} \Delta t$$

  Where:

  - $\beta = 1 \rightarrow Implicit$
  - $\beta = 0 \rightarrow Explicit$
  - $\beta = 0.5 \rightarrow Cranck - Nicolson$

- **Discretized equation**

  The discretization coefficients are evaluated for each internal node, according to the method chosen. Then, the boundary conditions are applied to boundary nodes and the relative coefficients are evaluated:

  - At $x = 0$, convection with the external temperature is modeled using a heat transfer coefficient α_{ext}.
  - At $x = e$, the boundary temperature is fixed at T_w.

- **TDMA Solver**

  The Tri-Diagonal Matrix Algorithm (TDMA) has been implemented to solve the system of linear equations for each time step, ensuring computational efficiency. Iterative convergence checks are applied to ensure stability and accuracy of the solution at each time step and a relaxation factor is implemented to help the solution converge more smoothly in the iterative method.

- **Convergence Check**

  Once the convergence is reached, the system proceeds computing temperatures at the next time step.

- **Evaluation of Temperature at each Instant**

  The model evaluates temperature evolution for 100 days, storing the temperature at:

  - $x = 0$ (exposed side).
  - $x = \frac{e}{2}$ (mid-wall).

    - $x = e$ (constant temperature boundary).

- **Outputs**

  The results are plotted to show:

    - Heat flux at $x = 0$ and $x = e$.
    - The temperature evolution at $x = 0$, $x = \frac{e}{2}$, and $x = e$.
    - Global energy balance.

Mesh Refinement Study

A mesh refinement study was conducted to ensure accurate and efficient results. A mesh with N=100 control volumes and a time step $\Delta t = 3600$ was chosen for its balance between resolution and computational efficiency. Larger N improves accuracy but increases computational time, while the chosen Δt showed stability in all integration methods but requires caution for explicit scheme. Relaxation factor improved convergence, especially with less refined mesh, helping to mitigate oscillations during iterative calculations.

Verification Test – Energy Balance

To ensure the correctness of the code, verification tests have been integrated to check the expected behavior of the solution under simplified or known conditions.

First a global energy balance is computed for each control volume by comparing the incoming and outgoing fluxes. The equation that ensures the conservation of energy for internal control volumes is:

$$EB_i = a_W[i]T[i-1] + a_E[i]T[i+1] + b_P[i] - a_P[i]T[i]$$

At the boundaries, the energy balances adapt to account for specific conditions:

- At $x = 0 \rightarrow EB_0 = a_E[0]T[1] + b_P[0] - a_P[0]T[0]$
- At $x = e \rightarrow EB_{N+1} = b_P[N+1] - a_P[N+1]T[N+1]$

The total energy balance for the entire domain is obtained by summing the local balances of all control volumes, including boundaries:

$$EB_{tot} = \sum_{i=0}^{N+1} EB_i$$

A total energy balance close to zero indicates that the numerical method has correctly conserved energy throughout the domain. This check is crucial for verifying the accuracy and reliability of the simulation. The energy balance has been evaluated from $t = 0$ to $t = 100 \times 24 \times 3600$, the result obtained is close to zero but not exactly zero due to numerical approximations and discretization errors. Key factors influenced this such as the mesh resolution Δx and the time step size Δt; tests were carried out with values higher than usual to allow the code to run in shorter times, leading to an Energy balance not exact but closer to zero by decreasing the time step.

Unsteady Schemes

The algorithm has been tested with all three unsteady schemes, Implicit, Explicit and Cranck-Nicolson. The Explicit method calculates the future state of the system directly from the current state, making it simple and computationally inexpensive, but it is conditionally stable and often requires very small time steps to avoid divergence. The Implicit method, in contrast, solves for the future state by forming and solving a system of equations, which is computationally more demanding but unconditionally stable, allowing for larger time steps. The Crank-Nicholson method strikes a balance by averaging explicit and implicit approaches, achieving second-order accuracy in both time and space while retaining unconditional stability. However, it also requires solving a system of equations at each time step, making it slightly more complex than the fully implicit method. The code was shot considering N=100 control volumes and a time step $\Delta t = 3600$ over a hundred days, to avoid high computational time, with the three different methods. Although the high time step, the explicit method didn't show instabilities, moreover, the implicit method didn't require much higher computational time than the others. Concluding that all three methods turned out to be suitable for the problem resolution.

Outputs

Finally, the energy exchanged at the boundaries has been plotted over time and showed in the following figure:

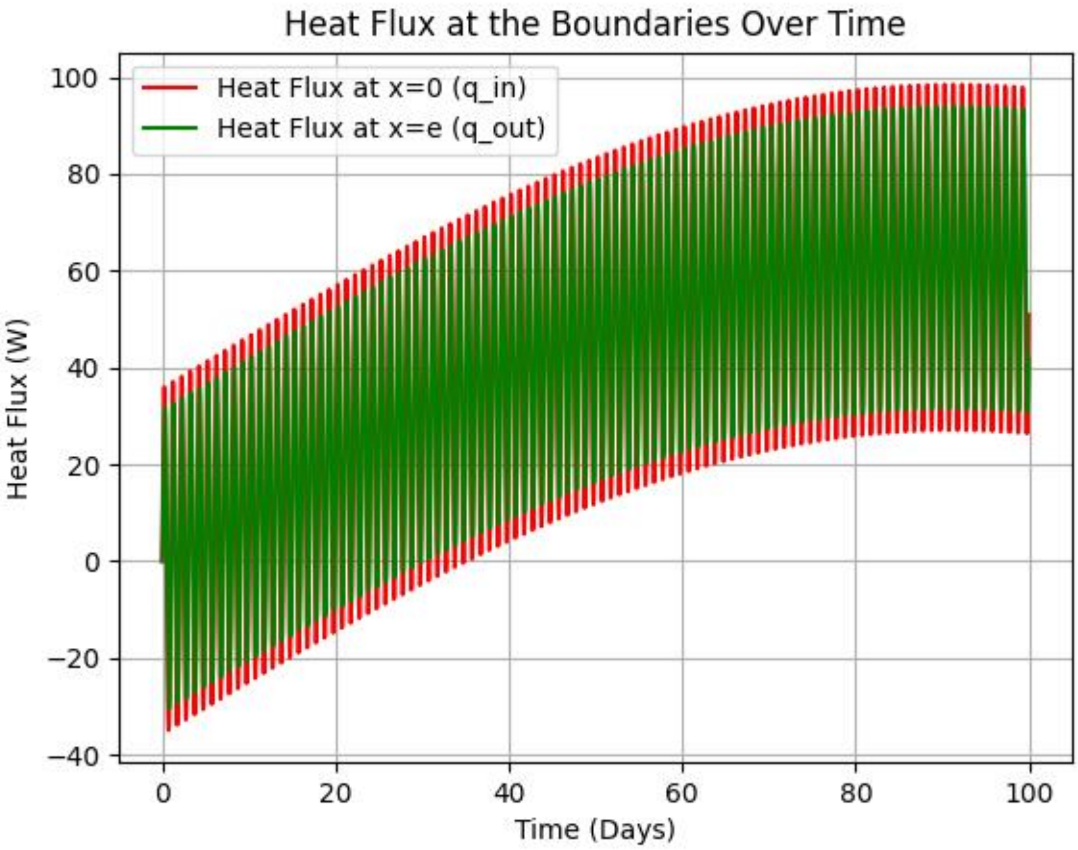

This graph shows the heat flux at the boundaries of the wall over 100 days. The red curve $\dot{q}_{in}$ represents the flux entering at $x = 0$, directly responding to the sinusoidal external temperature T_{ext}, while the green curve $\dot{q}_{out}$ represents the flux leaving at $x = e$, where the temperature is constant. $\dot{q}_{out}$ lags behind $\dot{q}_{in}$ and has a smaller amplitude, reflecting the effects of thermal resistance and diffusion through the wall. The slight upward trend in both fluxes indicates a growing average temperature gradient. This behavior validates the numerical model, capturing the expected phase lag and thermal response dynamics.

Then, the temperature evolution at specific positions of the wall have been evaluated and plotted over time.

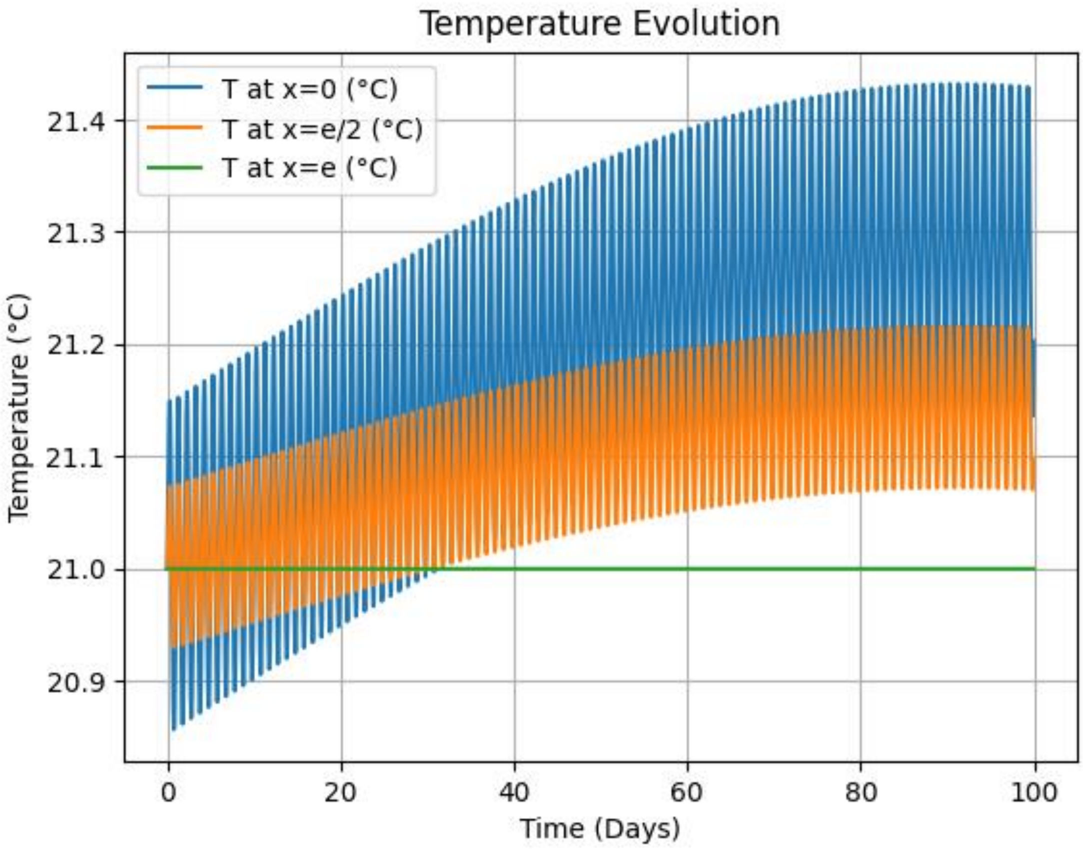

This graph shows the temperature evolution at different positions in the slab $x = 0, x = \frac{e}{2}, x = e$ over 100 days. The blue curve $T_{x=0}$ represents the temperature at the boundary exposed to the sinusoidal external temperature T_{ext} and closely follows its oscillations with the largest amplitude. The orange curve $T_{x=\frac{e}{2}}$ represents the mid-point temperature, which lags behind $T_{x=0}$ and shows a reduced oscillation amplitude due to the thermal resistance and diffusion within the wall. Finally, the green curve $T_{x=e}$ remains constant, as this boundary is maintained at a fixed temperature. The overall upward trend in the curves reflects the gradual increase in the average temperature gradient across the wall. This plot demonstrates the expected transient heat conduction behavior, showing attenuation and phase lag as heat propagates through the wall, which validates the numerical model.

Parametric Study

A parametric study was conducted to investigate the influence of key physical and numerical parameters on the transient heat conduction behavior of the wall. The parameters varied included wall thickness (e), thermal conductivity (λ), and external heat transfer coefficient (α_{ext}). For each parameter, simulations were performed over 100 days, and the Temperature have been printed at $x = 0, x = \frac{e}{2}, x = e$.

Table 2. Summary of parametric study results.

Parameter	Value	$T_{x=0}$ $[°C]$	$T_{x=\frac{e}{2}}$ $[°C]$	$T_{x=e}$ $[°C]$
Thickness	0.1	21.02	21.01	21.0
Thickness	1.0	21.20	21.10	21.0
Thickness	10.0	22.68	21.89	21.0
Conductivity	1.0	26.77	23.97	21.0
Conductivity	220.0	22.68	21.89	21.0
Conductivity	400.0	21.99	21.50	21.0
α_{ext}	0.0	21.00	21.00	21.0
α_{ext}	8.7	22.00	21.50	21.0
α_{ext}	60.0	24.21	22.51	21.0

Wall Thickness (e)

As the thickness increased from 0.1 m to 10.0 m, the temperature at $x = 0$ increased from 21.02 °C to 22.68 °C while the mid-point temperature $x = \frac{e}{2}$ increased from 21.01 °C to 21.89 °C. The temperature at $x = e$ remained fixed at 21.0°C as per the boundary condition. A thicker wall increased the thermal resistance, leading to a higher temperature gradient and reduced heat transfer rate.

Thermal Conductivity (λ):

Lower thermal conductivity ($\lambda = 1$) resulted in a significant temperature increase at $x = 0$ to 26.77 °C with minimal heat diffusion, keeping the mid-point temperature close to 24°C. Increasing λ to 400 W/m·K led to reduced temperature differences across the wall, with $T_{x=0} = 21.99\ °C$ and $T_{x=\frac{e}{2}} = 21.50\ °C$. This highlights the enhanced heat diffusion with higher conductivity.

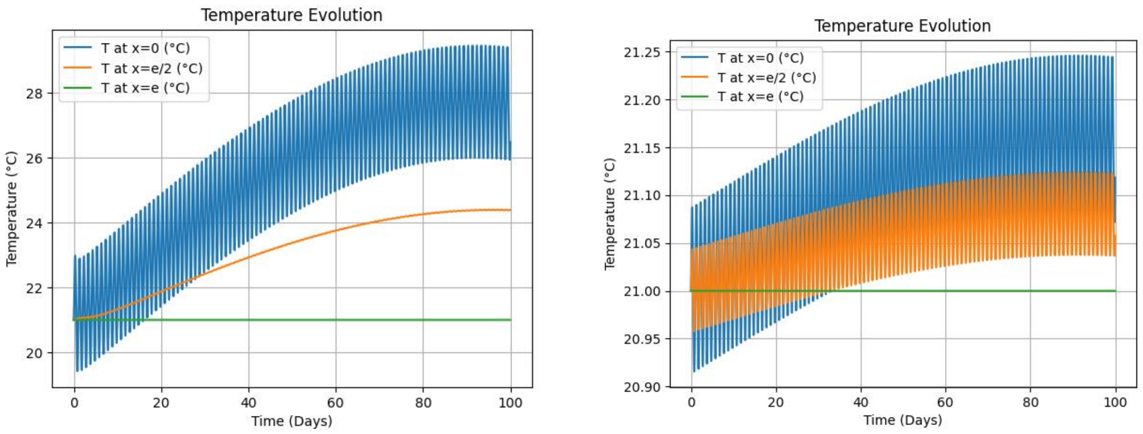

Figure 3. Temperature evolution with low thermal conductivity (left) and high conductivity (right).

External Heat Transfer Coefficient (α_{ext}):

A low $\alpha_{ext} = 0$ resulted in minimal heat exchange with the external environment, keeping the temperature at $x = 0$ near the initial temperature (21.0 °C). Increasing α_{ext} to 60 W/m²·K caused $T_{x=0}$ to rise to 24.21 °C and $T_{x=\frac{e}{2}}$ to 22.51 °C, indicating stronger thermal interaction with the oscillating external environment.

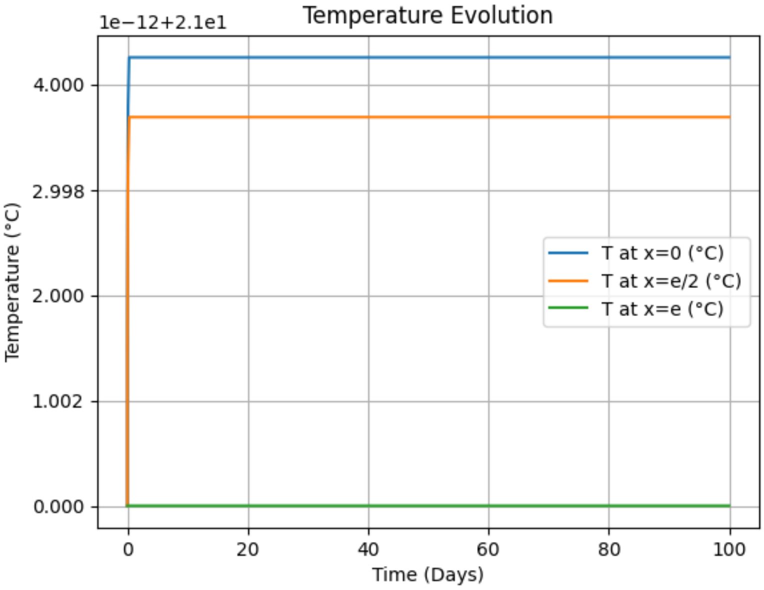

Figure 4. Temperature evolution with external convective coefficient equal to zero.

These results confirm the expected thermal behavior under varying parameters. Increased wall thickness and lower conductivity amplify thermal resistance, reducing heat transfer through the wall. Meanwhile, higher external heat transfer coefficients enhance the wall's response to external thermal oscillations. The study validates the model's ability to predict the thermal performance under diverse conditions and provides valuable insights into the thermal dynamics of the system.